Estimation of plant and canopy architectural traits using the D3P Digital Plant Phenotyping Platform

Shouyang Liu, Pierre Martre, Samuel Buis, Mariem Abichou, Bruno Andrieu, Frederic Baret

Plant Physiology Preview. Published on August 16, 2019, as DOI:10.1104/pp.19.00554

Breakthrough Technologies

Short title

High-throughput plant traits estimation using D3P

Author for Contact:

Shouyang Liu

LEPSE, Université Montpellier, INRA, Montpellier SupAgro, Montpellier, France

shouyang.liu@inra.fr

Frédéric Baret

INRA EMMAH, UMR 1114 Domaine Saint-Paul, Site Agroparc, Avignon, France

frederic.baret@inra.fr

Title

Estimation of plant and canopy architectural traits using the D3P Digital Plant Phenotyping Platform[1]

All author names and affiliations

Shouyang Liu[1, 2], Pierre Martre[2], Samuel Buis[1], Mariem Abichou[3], Bruno Andrieu[3] and Frédéric Baret[1]

[1] INRA EMMAH, UMR 1114 Domaine Saint-Paul, Site Agroparc, 84914 Avignon Cedex 9, France;

[2] LEPSE, Université Montpellier, INRA, Montpellier SupAgro, Montpellier, France;

Author contributions: S.L. and F.B. planned and designed the research. M.A and B.A. conducted the field experiment. S.B. contributed to the development of the assimilation method. S.L., F.B. and P.M. wrote the manuscript.
Corresponding authors: Shouyang Liu, shouyang.liu@inra.fr; Frédéric Baret, frederic.baret@inra.fr.
Funding: This work was supported by the "Infrastructure Biologie Santé" Phenome funded by the National Research Agency (ANR-11-INBS-0012). PM was also supported by the EU project H2020 SolACE (grant agreement no. 727247).

[3] INRA-AgroParisTech, UMR 1091 EGC, 78850 Thiverval-Grignon, France;

One sentence summary

The D3P Digital Plant Phenotyping Platform can be used to design and interpret phenotyping measurements for structural or functional trait extraction.

Abstract

The extraction of desirable heritable traits for crop improvement from high-throughput phenotyping (HTP) observations remains challenging. We developed a modeling workflow named Digital Plant Phenotyping Platform, D3P, to access crop architectural traits from HTP observations. D3P couples the ADEL (architectural model of development based on L-systems) wheat (*Triticum aestivum*) model, that describes the time course of the three-dimensional architecture of wheat crops, with simulators of images acquired with HTP sensors. We demonstrated that a sequential assimilation of the green fraction derived from RGB (Red Green Blue) images of the crop into D3P provides accurate estimates of five key parameters (phyllochron, lamina length of the first leaf, rate of elongation of leaf lamina, number of green leaves at the start of leaf senescence and minimum number of green leaves) of the ADEL-Wheat model that drive the time course of green area index and the number of axes with more than three leaves at the end of the tillering period. However, leaf and tiller orientation and inclination characteristics were poorly estimated. D3P was also used to optimize the observational configuration. The results, obtained from *in silico* experiments conducted on wheat crops at several vegetative stages, showed that the accessible traits could be estimated accurately with observations made at 0° and 60° zenith view inclination with a temporal frequency of 100 °Cd. This illustrates the potential of the proposed holistic approach that integrates all the available information into a consistent system for interpretation. The potential benefits and limitations of the approach are further discussed.

Introduction

Crop genetic improvement consists in selecting or creating the best performing genotypes under a set of environmental and management conditions (Bustos-Korts, 2017). Performances are mainly based on the quantity and quality of the harvested organs. Yield results from complex interactions between the genotype and the environment which makes direct selection based on yield very inefficient. It is preferred to identify an ensemble of structural and functional traits that are less dependent on the environment, explain part of the yield, and are strongly related to the genome (Hammer et al., 2006; Tardieu and Tuberosa, 2010; Rutkoski et al., 2016; Bustos-Korts, 2017). High-throughput phenotyping (HTP) is expected to provide such structural traits over a large collection of genotypes under contrasting climate and management scenarios. Further, the non-invasive nature of high-throughput phenotyping techniques allows repeat observations over time to possibly access functional traits.

High-throughput phenotyping (Paproki et al., 2012) accesses structural traits including lamina shape in wheat (*Triticum aestivum*) (Dornbusch and Andrieu, 2010), plant height (Hartmann et al., 2011; Madec et al., 2017), leaf angle (Cabrera Bosquet et al., 2016), plant density (Liu et al., 2016), ear density (Madec et al., 2019) or leaf area index (Liu et al., 2017). Three-dimensional (3D) reconstruction of the canopy may provide more details to access canopy structural traits and the functioning of the canopy (Gibbs et al., 2016). This technique has been applied on individual plants under well controlled illumination conditions by Duan et al. (2016), who used multi-view images to reconstruct 3D wheat structure at early stages and extract morphological traits. Its transposition to field conditions, where observations are generally only possible from the top, is still challenging as they provide an incomplete description of the 3D plant structure because of the occlusions inherent to vision techniques (Gibbs et al., 2016). A detailed and explicit description of the characteristics of each organ to better understand the crop functioning is still a pending question. Nevertheless, monitoring the plants from the top would allow to progressively build a description of the whole plant and infer the whole plant or stand characteristics. A dynamic plant architecture model will be very useful to keep a high degree of consistency between multidate observations, while providing sound assumptions on the fate of the organs at the bottom of the canopy that are partly occluded.

Functional Structural Plant Models (FSPMs) describe the detailed evolution of plant architecture with relatively simple environmental inputs, mainly air temperature and sowing patterns and a set of

parameters describing organ size, extension rate and topology (Vos et al., 2010). They can be coupled to radiative transfer models (RTM) such as Raytran (Govaerts and Verstraete, 1998) or LuxCoreRender (https://luxcorerender.org/) to simulate the corresponding 2D images acquired under a given observational geometry and waveband. The 3D nature of the FSPMs allows also simulating accurately the LiDAR (Light Detection And Ranging) signal. The FSPMs are thus able to link 2D (camera) or 3D (LiDAR) measurements by HTP techniques with plant level architectural traits corresponding to FSPM parameters. These parameters are expected to be more strongly associated to genomic regions than direct HTP measurements. This approach applied to single date observations corresponds to an advanced radiative transfer model inversion (Baret and Buis, 2008). It has been applied by Liu et al. (2017) to estimate the GAI (Green Area Index) over wheat crops from the combination of RGB (Red Green Blue) cameras and LiDAR observations. However, it did not exploit the temporal dimension that is described within FSPMs. Alternatively, comprehensive exploitation of multidate and/or multisensor observations to access FSPM parameters corresponds to a data assimilation approach that has been successfully applied to satellite observations (Moulin et al., 1998; Weiss et al., 2001; Bacour et al., 2015; Zhang et al., 2016). Data assimilation allows to integrate consistently into a single modeling workflow all information available including the phenotyping observations, environmental variables and the knowledge on the physical and biological processes integrated into FSPM and RTM. This approach benefits from the use of accumulated observations from several sensors and dates, which adds constraints in the parameter estimation process to get the set of optimal values (Combal et al., 2003; Baret and Buis, 2008). Consequently, more parameters of the FSPM can be estimated with increased accuracy. The resulting estimated parameters can then be used to derive emerging properties of the plant or the canopy such as the radiation interception efficiency.

The objective of this paper is to describe the potentials of such an assimilation approach for retrieving detailed plant and canopy characteristics from multidate observations of the GF (Green Fraction) that can be measured from RGB or multispectral imageries. The study focuses on wheat crops monitored from emergence to the end of the tillering period and is based on *in silico* experiments to demonstrate the feasibility of the proposed approach, avoiding possible limitations due to the realism of the models used, particularly the FSPM. It is based on the digital plant phenotyping platform (D3P) that was

specifically developed to simulate phenotyping measurements by coupling the ADEL (architectural model of development based on L-systems) wheat model (ADEL-Wheat) (Fournier et al., 2003) to the RTM, Persistence of Vision Raytracer (POV-Ray, Version 3.7). The D3P is first presented and then exploited to assimilate GF observations made at several dates and under several view directions to estimate 10 parameters of ADEL-Wheat. Finally, the approach is repeated for several temporal and directional samplings to select the optimal measurement configuration.

Results

Assimilation of green fraction into the Digital Plant Phenotyping Platform

In silico experiments were conducted using five view directions and five dates before tillering to estimate the five parameters of ADEL-Wheat $(\psi, L, \alpha_{leaf}, \Delta\varphi, \text{and } \Delta\theta)$ (**Table 1**) and GAI. We obtained very good estimates of ψ and L, even considering a noise of 10% on GF (**Fig. 1** and **Fig. 2**). Parameter α_{leaf} was retrieved with acceptable performances (**Fig. 2**). However, leaf orientation and inclination described by $\Delta\varphi$ and $\Delta\theta$ appeared difficult to retrieve from the dynamics of the directional GF before tillering (**Fig. 1** and **Fig. 2**). $\Delta\varphi$ determines the clumping of neighboring leaves with potentially substantial impact on the canopy light interception (Maddonni et al., 2001). The three first leaves are very small with little interactions between leaves of the same plant and almost no interactions between neighboring plants. This may explain why the azimuthal orientation pattern of leaves is not accessible from observations at the canopy scale during this early development phase.

The good retrieval performances of parameters driving the development of leaf area ($\psi, L, \text{and } \alpha_{leaf}$) explains the good estimation of GAI (**Fig. 1**). The retrieval performance of GAI is little affected by the noise associated with GF observations.

The sequential assimilation scheme proposed exploits observations before and during the tillering period to estimate five new parameters $(N_{\text{sen}}, N_{\min}, N_{\text{til}}, \theta_{\text{til}}, \text{and } \alpha_{\text{til}})$ (**Table 1**) while refining the five parameters estimated before tillering $(\psi, L, \alpha_{leaf}, \Delta\varphi, \text{and } \Delta\theta)$ (**Table 1**). Results show that adding the five observation dates during the second sub-period improves substantially the estimation of the first set of parameters (**Fig. 3**). The improvement was very large for ψ and α_{leaf}. For the parameters describing canopy architecture ($\Delta\varphi, \text{and } \Delta\theta$), the rRMSE (relative Root Mean Squared Error) was also drastically improved, particularly for the larger noise levels, but it was still higher than

0.5. The improvement was marginal for L, which was already well estimated using the first five dates before tillering. The impact of noise affecting GF observations on rRMSE for the first set of parameters was much reduced (**Fig. 3**). This was probably due to the multiplicity of the observations (10 dates, five directions) that smoothed out the random noise associated with GF.

Among the second set of parameters, N_{sen} that drives leaf senescence dynamics was relatively well estimated with rRMSE < 0.1 (**Fig. 3**). Conversely, $N_{\min}$ was more difficult to retrieve accurately with rRMSE ≈ 0.2 (**Fig. 3**). This can be explained by the fact that the influence of $N_{\min}$ on the dynamics of leaf senescence does not show up until the end of the tillering period, when the size of tillers is relatively small and partly hidden by the first leaves. The parameters driving the orientation of tillers ($\theta_{\text{tiller}}, \alpha_{\text{tiller}}$) were not retrieved accurately (**Fig. 3**). These parameters apply on tillers that are relatively small and partly hidden by the older leaves of the main stem. GAI was very well estimated, in agreement with the observations before tillering. In addition, d_{3l} was very well estimated.

Optimization of measurement configuration

The optimal measurement configuration is defined by the combination of dates and directions that provides the best retrieval performances for the three parameters ($\psi, L,$ and α_{leaf}) accessible before tillering in addition to GAI. Results showed that the average rRMSE on parameters ($\psi, L,$ and α_{leaf}) varies between 0.23 for GF observations from a single direction on a single date, down to 0.09 for the most comprehensive set of observations including the five dates and the five directions (**Fig. 4**). Best performances were obtained when at least three observation dates were used and when they were sufficiently distinct in time with the optimal case being dates [50, 150, 250] °Cd after crop emergence (**Fig. 4**). The multiplication of observation directions improved marginally the estimation of the parameters. For these early stages, Baret et al. (2010) already demonstrated that GF observed under 57° zenith angle provides an accurate estimate of GAI. Our results agree well with these findings, the best configurations always including a GF measurement at 60° zenith angle. The improvement when adding more directions might be mainly due to the reduction of the noise associated to the GF pseudo-measurements. Optimal performances were obtained when using two directions (0° and 60°) and three dates evenly distributed during the tillering period (**Fig. 4**). Adding more dates or directions improved only marginally the retrieval performances.

Discussion

Assimilation of green fraction observations provides accurate estimates of few pertinent wheat architectural traits

The green fraction is one of the most common canopy properties that can be derived from several high-throughput phenotyping sensors including RGB high resolution cameras (Guo et al., 2013), multispectral cameras based on vegetation indices (Comar et al., 2012), and radiative transfer model inversion (Li et al., 2015), as well as LiDAR systems (Liu et al., 2017). These devices can be installed aboard a range of possible vectors including fixed sensors at the ground level (Guo et al., 2013), semi-automatic light carts (White and Conley, 2013) or tractor based systems (Comar et al., 2012), fully automatic rover robots (Madec et al., 2017) running on the ground with active measurements, and unmanned aerial vehicles (Schirrmann et al., 2016). Our results clearly demonstrated that the assimilation of GF observations provide accurate estimates of the few ADEL-Wheat parameters that drive the dynamics of GAI: the phyllochron, ψ, the lamina length of the first leaf, L, the rate of elongation of leaf lamina, α_{leaf}, the number of green leaves at the start of leaf senescence, N_{sen}, and the minimum number of green leaves, N_{min}. The phyllochron that varies among cultivars (Hay and Kirby, 1991; He et al., 2012) is of high interest. The phyllochron describing leaf appearance rate responds non-linearly to multi-environmental factors. When it is modeled using only temperature, residual environmental-effects are often observed (Cao and Moss, 1989; Baumont et al., 2019). This can be partly removed using the photothermal time corresponding to temperatures accumulated during the light time period only (Masle et al., 1989). Environmental factors may have also substantial effects on the final length of leaves, L. Therefore, the influence of the environmental conditions on ψ and L should be explicitly modeled into ADEL-Wheat to characterize the early plant vigor that is a very pertinent trait to be selected (Edmeades, 1996; Monneveux et al., 2012). Parameter α_{leaf} that drives the lamina length of successive leaves may be also a good proxy of the early plant vigor. Parameters N_{sen} and N_{min} are traits of potential interest for drought tolerance (Araus et al., 1997; Hafsi et al., 2007). Conversely, parameters related to leaf or tiller orientation were poorly retrieved either because they vary within relatively narrow ranges or because they apply to organs with limited area or hidden by other organs. Nevertheless, the good estimates of $(\psi, L, \alpha_{leaf}, N_{\mathrm{sen}}, \mathrm{and}\, N_{\mathrm{min}})$ parameters that drive the dynamics of GAI allows simulating accurately GAI continuously with a rRMSE < 0.05.

Baret et al. (2010) demonstrated that GAI could be estimated with an rRMSE of 0.12 using single green fraction measurements from 57.5° zenith angle when leaves are assumed randomly distributed in the canopy. The improved performances shown here comes from the additional information used in the assimilation scheme, with more directions and more dates of observations. Further, our assimilation method ensures to get a consistent time course of GAI before tillering using the temporal constraints provided by the dynamic ADEL-Wheat model. In addition to GAI, d_{3l}, the number of axes with more than three leaves, was accurately computed from the estimated parameters $(\psi, L, \alpha_{leaf}, N_{\mathrm{sen}}, \text{and } N_{\min})$. This trait is commonly used as a proxy of ear density and thereby of potential yield as tillers having three leaves at the start of stem elongation continue to grow and generally complete their development and produce an ear (Nerson, 1980; Whaley et al., 2000). Conversely, the other tillers generally regress due to the competition between neighboring tillers and plants (Masle, 1985).

Assimilation exploits consistently all the available information into a single workflow

The assimilation approach that integrates multidate remote sensing observations into process models, was originally developed for satellite observations (Moulin et al., 1998; Weiss et al., 2001; Bacour et al., 2015; Zhang et al., 2016). It was applied here to HTP measurements. Data assimilation offers several advantages as compared to the more classical crop characteristics retrieval approaches. First, it integrates into a single and consistent workflow all the available information including phenotyping observations, environmental variables and knowledge on the physical and biological processes embedded in the FSPM and RTM. Second, it capitalizes on the accumulation of observations from several sensors and dates and thereby facilitates the parameter estimation process (Baret and Buis, 2008; Combal et al., 2003). Third, data assimilation within such a modelling workflow permits to access plant and canopy level architectural properties that cannot be directly measured in the field at high throughput. Finally, the combination of ADEL-Wheat with simulators of several phenotyping measurements allows assimilating concurrently observations coming from different sensors. This will allow adding more information in the interpretation system to provide more accurate parameter estimates or new traits.

Optimizing of the measurement configuration

The proposed approach allows defining the optimal measurement configuration that provides a trade-off between the accuracy of trait estimation and the cost/time associated to the multiplication of measurements and devices. This was demonstrated here by selecting the more parsimonious combination of dates and directions of observations. Results show that observations made at 0° and 60° and repeated every 100 °Cd provide the best estimates of the accessible traits. The optimization process allows playing on additional elements of the measurement configuration including the uncertainties associated to the measurements, the spatial resolution, or the interest of additional devices.

Potential benefits and limitations of the assimilation technique

The sequential assimilation scheme proposed here splits the retrieval problem into sub-problems. It gradually adds parameters to be estimated as soon as they are required, limiting the complexity of the problem (Baret and Buis, 2008). Further, the values of the parameters needed for the first stages can be refined when exploiting later observations since they affect the fate of the canopy for the later growth stages. For the sake of simplicity, we focused on early growth stages that are recognized to be critical for the implantation of the crop and the competition with weeds. The traits estimated are therefore considered crucial to identify cultivars with higher early vigor and competitiveness with weeds or other crops/genotypes (Araus et al., 1997; Hafsi et al., 2007). However, the approach could be also applied to later stages to capture additional traits. This will be achieved at the expense of increased complexity because of the growing number of parameters to be considered. Additionally, our simulations are based on fixed thermal time and directions under which the GF are observed. However, the dynamics of GF is smooth since it results from incremental growth and senescence processes. Therefore, it would be possible to interpolate the GF values between the fixed dates simulated in this exercise to match the actual dates. Similar smooth variations of GF are expected as a function of the directions of GF observations. Therefore, it would also be possible to interpolate between the fixed directions to match the actual ones under which GF is observed.

The results presented here were based on *in silico* experiments where pseudo-observations were used instead of actual measurements. This probably boosts artificially the retrieval performances since the consistency of the ADEL-Wheat model with the actual canopy structure development was not challenged. The assimilation approach should therefore be further evaluated using actual observations

to ensure that the possible systematic error on the description of the dynamics of canopy structure by the ADEL-Wheat model is limited. Nonetheless, the noise added on the GF observations demonstrates that the approach is relatively robust to random error thanks to the multiplicity of the observations.

The performances of the proposed approach when applied to actual observations rely on the realism of the FSPM, ADEL-Wheat in our case. In a previous work, we pointed out the limits of ADEL-Wheat to get realistic GF values acquired close to nadir directions because of the possible interactions between leaves at early growth stages that were not always accurately described (Liu et al., 2017). However, it is possible to use only inclined observations for these early stages, which would limit the impact of model approximations on the estimation of the model parameters. Besides, ADEL-Wheat assumes that tillering ceases when the first internode starts to elongate (Kirby et al., 1985). However, the end of tillering can be strongly affected by external factors including light quality within the canopy (Evers et al., 2006) and photoperiod (Miralles and Richards, 2000). Although simplifications and assumptions on the description of some processes are always necessary, phenotyping observations will contribute to provide the required information for improving the realism of FSPMs.

As in many FSPMs, ADEL-Wheat incorporates very little functioning in terms of ecophysiological processes, which limits the type of traits that can be extracted by assimilating phenotyping observations into D3P. The next step should be to retrieve crop growth model parameters describing canopy response to environmental factors, i.e. truly functional traits, from the assimilation of the structural parameters retrieved from the proposed combination of high-throughput phenotyping observations and D3P. Some wheat crop growth models such as *SiriusQuality* (Martre and Dambreville, 2018) describes the leaf area dynamics from the growth of individual leaves and tillers using an approach similar to that of ADEL-Wheat. In order to feed a crop model such as *SiriusQuality* with the FSPM parameters, they should be reparametrized so that the retrieved parameters have the same meaning in both models. Parameters determining the short-term responses of physiological processes to environmental factors are now also accessible in HTP platforms (Prado et al., 2018), which can limit the number of parameters that need to be retrieved by data assimilation.

Materials and Methods

Description of the digital plant phenotyping platform

The digital plant phenotyping platform (D3P) includes two components: a 3D canopy structure model and simulators of the phenotyping observations from LiDARs and multispectral or RGB cameras (**Fig. 5**). Three-dimensional canopy structures were simulated using the FSPM modeling platform OpenAlea (Pradal et al., 2008). OpenAlea is used in D3P to create 3D meshes of virtual canopies. LiDAR data are simulated using the 3D crop modelling library Plantgl (Pradal et al., 2009). Multispectral and RGB images are simulated using the Persistence of Vision Raytracer (POV-Ray, Version 3.7), which renders complex 3D scenes for a range of camera specifications. Optical properties of plant organs are simulated with the PROSPECT model (Jacquemoud and Baret, 1990) using the Python library PyProSAIL. RGB simulator is a special case of multispectral camera for red, green, and blue channels. By defining the sensor properties and the observational configuration (Supporting Information **Supplemental Table S1**), we can mimic with a very high realism any phenotyping measurement (**Supplemental Video S1**).

The accuracy of the LiDAR simulator has been previously evaluated through comparison with LiDAR measurements (Liu et al., 2017). The performance of POV-Ray based radiative transfer simulation was evaluated through radiation transfer model inter-comparison using an on-line model checker, ROMC (Widlowski et al., 2008). The evaluation of POV-Ray (in **Supplemental Figure S1)** shows satisfactory results.

D3P is programmed in Python. All D3P dependencies are open-source and their code is accessible from the code repositories and websites given in **Table S2**. The code and user manual of D3P is freely available in GitHub (https://github.com/lsymuyu/Digital-Plant-Phenotyping-Platform). DP3 is distributed under the free software open source license MIT.

Simplification of ADEL-Wheat functional-structural plant model

Virtual wheat (*Triticum aestivum*) canopies were simulated with the wheat FSPM ADEL-Wheat implemented in OpenAlea (Fournier and Andrieu, 1999; Abichou et al., 2013; Liu et al., 2017). Plant development is primarily driven by temperature and the thermal time between the appearance of two successive leaf tips, i.e. the phyllochron. The phyllochron is considered constant from seedling to flag leaf expansion (Hokmalipour, 2011). The current version of ADEL-Wheat needs more than 50 parameters to describe explicitly the dimension, orientation and inclination of each organ (for a

detailed presentation of ADEL-Wheat see http://openalea.gforge.inria.fr/doc/alinea/adel/doc/_build/html/user/manual.html). Therefore, a reduced number of parameters was required in order to estimate them from HTP observations. We reparametrized the leaf dimension representation in ADEL-Wheat using a large dataset covering 28 winter wheat experiments conducted over several years in Grignon, France, with a range of sowing dates, cultivars, and nitrogen levels (Abichou, 2016). The modifications proposed are detailed in Supplemental Methods S1. A total of 10 influential parameters controlling the canopy development from emergence to the beginning of stem elongation was finally necessary to drive the simplified version of ADEL-Wheat model. Before tillering starts, i.e. before ligulation of the third leaf on the main stem (Masle, 1985), five parameters drive the plant structure dynamics (**Table 1**):

- The phyllochron, ψ, controls the time of leaf appearance and the rate of leaf extension;
- The lamina length of the first three leaves is assumed to change linearly with leaf rank. It is parameterized by the lamina length of the first leaf L and the slope, α_{leaf}, of the relationship between lamina length and leaf rank;
- Leaf orientation is initialized from the seedling stage depending on seed orientation. Seeds are assumed to be sown with a random azimuth (Ledent and Moss, 1977). Evers et al. (2005) found that the azimuth of successive leaves is mainly opposite for the first three leaves. The azimuth angle of a leaf relative to the previous one was drawn from a Gaussian distribution with mean angle of 180° and standard deviation $\Delta\varphi$ accounting for the plasticity of the cultivar. The leaf inclination was described based on experimental observations (Abichou, 2016). Variations of leaf inclination is controlled by the basal inclination, $\Delta\theta$.

During the tillering phase, i.e. between ligulation of the third leaf on the mainstem and the beginning of stem elongation (Abichou et al., 2018), five additional parameters drive tiller development and leaf senescence (**Table 1**):

- Leaf senescence is described by the number of green leaves on the mainstem when senescence starts, N_{sen}, and the minimum number of green leaves on the mainstem, N_{min} (Abichou et al., 2013);
- Final number of tillers, N_{til};
- Leaf inclination, θ_{til};

- Change of tiller inclination angle with the number of visible leaves, α_{til}.

Simulation of synthetic datasets

We simulated RGB images of wheat canopies using D3P with our simplified version of ADEL-Wheat. We rendered 2 × 2 m scenes containing 11 rows with and inter-row spacing of 17.5 cm and a sowing density of 250 seeds·m^{-2}. Note that plant density was not considered as an unknown parameter since high resolution RGB imagery techniques have been developed to accurately measure it and document the associated sowing pattern (Jin et al., 2017; Liu et al., 2017). A total of 2,500 combinations of the five influential parameters of ADEL-Wheat before tillering (**Table 1**) were randomly drawn using a Latin Hypercube sampling scheme. The parameters were assumed to follow a uniform distribution within their range of variation (Abichou, 2016; **Table 1**). During tillering, a similar sampling strategy was used for the five influential parameters during that period (**Table 1**). The canopies were simulated every 50 °Cd before tillering (between 50 and 250 °Cd after crop emergence) and every 100 °Cd during tillering (between 300 and 700 °Cd after crop emergence).

GF in a given direction is defined as the fraction of green elements viewed in this particular direction. It is computed from the classification of RGB images. The RGB camera with a ±10° field of view was placed at 1.5 m above the canopy, providing a footprint of 50 × 50 cm. The images had a resolution of 500 × 500 pixels with a 1 mm spatial resolution, which appears to be a good compromise between computation time and performances. Marginal classification errors were expected in the calculation of GF from our simulations. Noise was thus added to the simulated GF values to mimic the actual GF measurements where possible classification errors may be observed due to confusions between green vegetation and non-green elements or the soil surface, depending on illumination conditions and camera spatial resolution. We assumed that the noise followed a Gaussian distribution with a mean of zero and a standard deviation of 0.05 and 0.10, which are typical values (Baret et al., 2010; Liu et al., 2017). We then rendered the 3D scenes using POV-Ray every 15° between 0° and 60°. View azimuth was perpendicular to the row to maximize the sensitivity to canopy structure (López-Lozano et al., 2007; Lopez-Lozano et al., 2009).

GF was computed for the 10 dates and the five view directions for each of the 2,500 combinations of ADEL-Wheat parameters (**Table 1**). The 125, 000 simulated RGB images and corresponding GF

values will be called 'pseudo-observations' in the following (illustrated in **Supplemental Figure S2**). Each of the 2,500 input parameter combination were also associated to two additional traits: the GAI at each of the 10 dates and the number of axes with more than three leaves (d_{3l}) at the end of the tillering period. Training and validation processes were conducted with 85% and 15% of the synthetic dataset, respectively.

Green fraction assimilation

The assimilation process was conducted sequentially for the two growth periods as illustrated in **Fig. 6**. The five parameters involved before tillering ($\psi, L, \alpha_{\mathrm{leaf}}, \Delta\varphi,$ and $\Delta\theta$) were first estimated. Then the five additional parameters required for the tillering period ($N_{sen}, N_{\min}, N_{\mathrm{til}}, \theta_{\mathrm{til}}$ and α_{til}) were estimated while the first five parameters were fine-tuned since they also influence the architecture of canopies during tillering. In the second assimilation step, GF data from crop emergence to beginning of stem elongation were also assimilated.

For each of the two periods, the assimilation process consisted in adjusting the ADEL-Wheat parameters (**Table 1**) to get a good agreement between the simulated GF and the GF pseudo-observations for the 10 dates and five directions considered. Parameter adjustment was completed using a neural network (NN) machine learning approach, which is well adapted to our case where the simulations are time consuming, preventing from using iterative optimization approaches (Kimes et al., 2000; Baret and Buis, 2008). We used a one-layer feed-forward network with tangent sigmoid transfer functions in the first layer and a linear transfer function in the output layer. The number of neurons in the hidden layer is based on the geometric pyramid rule proposed by Masters (1993). The optimal number of neurons in the hidden layer should be close to $\sqrt{nm}$ with n and m being the number of inputs and outputs, respectively. Then the synaptic weights and biases are tuned using the Levenberg-Marquardt optimization algorithm (Marquardt and Mathematics, 1963) to best match the output values over the training database. The accuracy of the estimated parameters was assessed with the relative root mean squared error (rRMSE).

Defining the optimal observational configuration

The optimal measurement configuration for the retrieval of plant and canopy architectural traits was investigated using D3P. We analyzed, among the 961 possible combinations of five dates and five

directions, the ones providing the best retrieval performances for the ADEL-Wheat parameters and GAI. Pseudo measurements of GF were assimilated into D3P using the trained NN for each of the 961 configurations considered the same way as described above for the five dates and five directions. A 5% Gaussian noise was applied on GF values simulated by D3P. Retrieval performances were quantified as the average rRMSE computed on the targeted traits and GAI for validation dataset (375 among the 2,500 combinations of the parameters presented in **Table 1**). For GAI, the rRMSE was computed for the five dates before tillering.

Supporting Information

Supplemental Methods S1. Description of the simplified ADEL-Wheat model.

Supplemental Figure S1. Comparison between the reflectance simulations (named 'Canray') and the corresponding reference values.

Supplemental Figure S2. RGB (Red Green Blue) and the corresponding binary imagery of virtual wheat canopies simulated with the Digital Plant Phenotyping Platform.

Supplemental Figure S3. Reparameterization of leaf dimension representation in ADEL-Wheat model.

Supplemental Video S1. Digital Plant Phenotyping Platform mimicking unmanned aerial vehicle flight over wheat canopies.

Supplemental Table S1. Input parameters of LiDAR and multispectral/RGB simulators for the Digital Plant Phenotyping Platform.

Supplemental Table S2. Name and code repository of the Digital Plant Phenotyping Platform software and library dependencies.

Acknowledgements

We are grateful to Christian Fournier and Christophe Pradal for their help in the use of the ADEL-Wheat model and the OpenAlea platform. We also thank Jingyi Jiang for her help in accomplishing the radiation transfer model inter-comparison test.

Table

Table 1 Influential parameters of the simplified ADEL-Wheat model estimated in the Digital Plant Phenotyping Platform. The range of variation as observed in field experiments is indicated (Abichou, 2016).

Growth period	Name	Descriptions	Value		Unit
			Min	Max	
Before tillering	ψ	Phyllochron	80	120	°Cd
	L	Laminae length of leaf 1, rank from the bottom	4	8	cm
	α_{leaf}	Increase rate of lamina length	-3	3	cm phytomer^{-1}
	$\Delta\varphi$	Standard deviation of the leaf azimuth compared to the previous one with mean 180°	0	90	°
	$\Delta\theta$	Shift of leaf basal inclination	-15	15	°
During tillering	N_{sen}	Number of green leaves at the start of leaf senescence on the mainstem	3.5	6.5	leaves
	N_{min}	Minimum number of green leaves on the mainstem	1.5	3.5	leaves
	N_{til}	Final number of tillers per plant	0	5	tillers
	θ_{til}	Inclination of the base of tillers relative to mainstem inclination	10	85	°
	α_{til}	Change of tiller inclination angle with the number of emerged leaves	10	50	° Haun stage^{-1}

List of Figure legends

Fig. 1 Relative root mean squared error (rRMSE) for five parameters of ADEL-Wheat and green area index (GAI) estimated with the Digital Plant Phenotyping Platform using the green fraction observations under five view directions for five dates before tillering. Three levels of noise were considered (0%, 5% and 10%) for the evaluation dataset. The five parameters are: ψ, phyllochron; L, laminae length of leaf 1, rank from the bottom; α_{leaf}, increase rate of lamina length; $\Delta\varphi$, standard deviation of the leaf azimuth compared to the previous one with mean 180°; $\Delta\theta$, shift of leaf basal inclination.

Fig. 2 Comparison of the estimated and pseudo-observation values of the five parameters of ADEL-Wheat and the green area index (GAI) computed for the five dates of green fraction (GF) measurements with the reference values for the first growth period (between crop emergence and ligulation of leaf 3). Synthetic GF data were obtained from five view directions with 5% noise. The five parameters are: N_{sen}, number of green leaves at the start of leaf senescence on the mainstem; N_{min}, minimum number of green leaves on the mainstem; N_{til}, final number of tillers per plant; θ_{til}, inclination of the base of tillers relative to mainstem inclination; α_{til}, change of tiller inclination angle with the number of emerged leaves.

Fig. 3 Relative root mean squared error (rRMSE) for ten parameters of ADEL-Wheat, green area index (GAI), and the number of tillers with at least three leaves at the beginning of stem elongation (d_{3l}) estimated with the Digital Plant Phenotyping Platform using the green fraction observations under five view directions for 10 dates between crop emergence and the beginning of stem elongation. Three levels of noise were considered (0%, 5% and 10%) for the evaluation dataset. The ten parameters include: ψ, phyllochron; L, laminae length of leaf 1, rank from the bottom; α_{leaf}, increase rate of lamina length; $\Delta\varphi$, standard deviation of the leaf azimuth compared to the previous one with mean 180°; $\Delta\theta$, shift of leaf basal inclination N_{sen}, number of green leaves at the start of leaf senescence on the mainstem; N_{min}, minimum number of green leaves on the mainstem; N_{til}, final number of tillers per plant; θ_{til}, inclination of the base of tillers relative to mainstem inclination; α_{til}, change of tiller inclination angle with the number of emerged leaves.

Fig. 4 Average relative root mean squared error (rRMSE) for the three estimated ADEL-Wheat parameters ($\psi, L,$ and α_{leaf}) and GAI obtained from the 961 combinations of one to five directions and one to five dates before tillering.

Fig. 5 Schema of the Digital Plant Phenotyping Platform (D3P) that simulates phenotyping observations from environmental variables, crop management and meteorological information.

Fig. 6 Diagram showing the sequential scheme of green fraction assimilation. The assimilation was done in two consecutive steps: between crop emergence and the start of tillering (before tillering), and between crop emergence and the beginning of stem elongation (before stem elongation). In each step, a neural network (NN) was first trained using the training green fraction (GF(t,Ω)) dataset. The trained NN was then used to estimate ADEL-Wheat parameters and GAI using the green fraction (GF(t,Ω)) validation dataset. The distribution of ADEL-Wheat parameters estimated in the first step (before tillering) were used as prior information when training the NN in the second step (before stem elongation). Finally, the tiller number with more than three leaves at the beginning of stem elongation (d_{3l}) was computed from the estimated set of parameters.

Literature Cited

Abichou M (2016) Modélisation de l'architecture 4D du blé : identification des patterns dans la morphologie, la sénescence et le positionnement spatial des organes dans une large gamme de situations de croissance. AgroParisTech, Université Paris-Saclay, Paris

Abichou M, Fournier C, Dornbusch T, Chambon C, Baccar R, Bertheloot J, Vidal T, Robert C, David G, Andrieu B (2013) Re-parametrisation of Adel-wheat allows reducing the experimental effort to simulate the 3D development of winter wheat. *In* Proceedings of the 7th International Conference on Functional-Structural Plant Models, pp 304–306

Abichou M, Fournier C, Dornbusch T, Chambon C, de Solan B, Gouache D, Andrieu B (2018) Parameterising wheat leaf and tiller dynamics for faithful reconstruction of wheat plants by structural plant models. Field Crops Research **218:** 213-230

Araus J, Amaro T, Zuhair Y, Nachit M (1997) Effect of leaf structure and water status on carbon isotope discrimination in field grown durum wheat. Plant, Cell & Environment **20:** 1484-1494

Bacour C, Peylin P, MacBean N, Rayner PJ, Delage F, Chevallier F, Weiss M, Demarty J, Santaren D, Baret F, Berveiller D, Dufrene E, Prunet P (2015) Joint assimilation of eddy covariance flux measurements and FAPAR products over temperate forests within a process-oriented biosphere model. Journal of Geophysical Research-Biogeosciences **120:** 1839-1857

Baret F, Buis S (2008) Estimating canopy characteristics from remote sensing observations: Review of methods and associated problems. *In* Advances in land remote Sensing. Springer, pp 173–201

Baret F, de Solan B, Lopez-Lozano R, Ma K, Weiss M (2010) GAI estimates of row crops from downward looking digital photos taken perpendicular to rows at 57.5° zenith angle: Theoretical considerations based on 3D architecture models and application to wheat crops. Agricultural and Forest Meteorology **150:** 1393-1401

Baumont M, Parent B, Manceau L, Brown H, Driever SM, Muller B, Martre P (2019) Experimental and modeling evidence of carbon limitation of leaf appearance rate for spring and winter wheat. Journal of Experimental Botany **70:** 2449-2462

Bustos-Korts D (2017) Modelling of genotype by environment interaction and prediction of complex traits across multiple environments as a synthesis of crop growth modelling, genetics and statistics. Wageningen University, Wageningen

Cabrera Bosquet L, Fournier C, Brichet N, Welcker C, Suard B, Tardieu F (2016) High throughput estimation of incident light, light interception and radiation use efficiency of thousands of plants in a phenotyping platform. New Phytologist **212:** 269-281

Cao W, Moss DN (1989) Temperature and daylength interaction on phyllochron in wheat and barley. Crop Science **29:** 1046–1048

Comar A, Burger P, de Solan B, Baret F, Daumard F, Hanocq JF (2012) A semi-automatic system for high throughput phenotyping wheat cultivars in-field conditions: description and first results. Journal of Functional Biology **39:** 914-924

Combal B, Baret F, Weiss M, Trubuil A, Macé D, Pragnère A, Myneni R, Knyazikhin Y, Wang L (2003) Retrieval of canopy biophysical variables from bidirectional reflectance. Remote Sensing of Environment **84:** 1-15

Dornbusch T, Andrieu B (2010) Lamina2Shape—An image processing tool for an explicit description of lamina shape tested on winter wheat (Triticum aestivum L.). Computers and Electronics in Agriculture **70:** 217-224

Duan T, Chapman S, Holland E, Rebetzke G, Guo Y, Zheng B (2016) Dynamic quantification of canopy structure to characterize early plant vigour in wheat genotypes. Journal of Experimental Botany **67:** 4523-4534

Edmeades GO (1996) Developing Drought and Low N-tolerant Maize: Proceedings of a Symposium, March 25-29, 1996, CIMMYT, El Batán, Mexico. CIMMYT

Evers JB, Vos J, Andrieu B, Struik PC (2006) Cessation of tillering in spring wheat in relation to light interception and red : far-red ratio. Annals of Botany **97:** 649-658

Evers JB, Vos J, Fournier C, Andrieu B, Chelle M, Struik PC (2005) Towards a generic architectural model of tillering in Gramineae, as exemplified by spring wheat (Triticum aestivum). New Phytologist **166:** 801-812

Fournier C, Andrieu B (1999) ADEL-maize: an L-system based model for the integration of growth processes from the organ to the canopy. Application to regulation of morphogenesis by light availability. Agronomie **19:** 313–327

Fournier C, Andrieu B, Ljutovac S, Saint-Jean S (2003) ADEL-wheat: a 3D architectural model of wheat development. Proceedings of the 2003 Plant Growth Modeling, Simulation, Visualization, and Applications**:** 54–63

Gibbs JA, Pound M, French AP, Wells DM, Murchie E, Pridmore T (2017) Approaches to three-dimensional reconstruction of plant shoot topology and geometry. Functional Plant Biology **44:** 62-75

Govaerts YM, Verstraete MM (1998) Raytran: A Monte Carlo ray-tracing model to compute light scattering in three-dimensional heterogeneous media. Ieee Transactions on Geoscience and Remote Sensing **36:** 493-505

Guo W, Rage UK, Ninomiya S (2013) Illumination invariant segmentation of vegetation for time series wheat images based on decision tree model. Computers and Electronics in Agriculture **96:** 58-66

Hafsi M, Akhter J, Monneveux P (2007) Leaf senescence and carbon isotope discrimination in durum wheat (Triticum durum Desf.) under severe drought conditions. Cereal Research Communications **35:** 71-80

Hammer G, Cooper M, Tardieu F, Welch S, Walsh B, van Eeuwijk F, Chapman S, Podlich D (2006) Models for navigating biological complexity in breeding improved crop plants. Trends in Plant Science **11:** 587-593

Hartmann A, Czauderna T, Hoffmann R, Stein N, Schreiber F (2011) HTPheno: an image analysis pipeline for high-throughput plant phenotyping. BMC bioinformatics **12:** 148

Hay R, Kirby E (1991) Convergence and synchrony-a review of the coordination of development in wheat. Crop and Pasture Science **42:** 661-700

He J, Le Gouis J, Stratonovitch P, Allard V, Gaju O, Heumez E, Orford S, Griffiths S, Snape JW, Foulkes MJ, Semenov MA, Martre P (2012) Simulation of environmental and genotypic variations of final leaf number and anthesis date for wheat. European Journal of Agronomy **42:** 22-33

Hokmalipour S (2011) The Study of Phyllochron and Leaf Appearance Rate in Three Cultivar of Maize (Zea mays L.) At Nitrogen Fertilizer Levels. World Applied Sciences Journal **12:** 850–856

Jacquemoud S, Baret F (1990) PROSPECT: A model of leaf optical properties spectra. Remote sensing of environment **34:** 75-91

Jin X, Liu S, Baret F, Hemerlé M, Comar A (2017) Estimates of plant density of wheat crops at emergence from very low altitude UAV imagery. Remote Sensing of Environment **198:** 105-114

Kimes DS, Knyazikhin Y, Privette JL, Abuelgasim AA, Gao F (2000) Inversion methods for physically-based models. Remote Sensing Reviews **18:** 381-439

Kirby EJM, Appleyard M, Fellowes G (1985) Leaf emergence and tillering in barley and wheat. Agronomie **5:** 193–200

Ledent JF, Moss DN (1977) Spatial orientation of wheat leaves. Crop Science **17:** 873–879

Li W, Weiss M, Waldner F, Defourny P, Demarez V, Morin D, Hagolle O, Baret F (2015) A Generic Algorithm to Estimate LAI, FAPAR and FCOVER Variables from SPOT4_HRVIR and Landsat Sensors: Evaluation of the Consistency and Comparison with Ground Measurements. Remote Sensing **7:** 15494-15516

Liu S, Baret F, Abichou M, Boudon F, Thomas S, Zhao K, Fournier C, Andrieu B, Irfan K, Hemmerlé M, de Solan B (2017) Estimating wheat green area index from ground-based LiDAR measurement using a 3D canopy structure model. Agricultural and Forest Meteorology **247:** 12-20

Liu S, Baret F, Andrieu B, Abichou M, Allard D, de Solan B, Burger P (2017) Modeling the spatial distribution of plants on the row for wheat crops: Consequences on the green fraction at the canopy level. Computers and Electronics in Agriculture **136:** 147-156

Liu S, Baret F, Andrieu B, Burger P, Hemmerle M (2017) Estimation of Wheat Plant Density at Early Stages Using High Resolution Imagery. Frontiers in Plant Science **8:** 739

López-Lozano R, Baret F, Chelle M, Rochdi N, España M (2007) Sensitivity of gap fraction to maize architectural characteristics based on 4D model simulations. Agricultural and Forest Meteorology **143:** 217-229

Lopez-Lozano R, Baret F, García de Cortázar-Atauri I, Bruguier N, Casterad MA (2009) Optimal geometric configuration and algorithms for LAI indirect estimates under row canopies. The case of vineyards. Agricultural and Forest Meteorology **149:** 1309-1316

Maddonni GA, Chelle M, Drouet JL, Andrieu B (2001) Light interception of contrasting azimuth canopies under square and rectangular plant spatial distributions: simulations and crop measurements. Field Crops Research **70:** 1-13

Madec S, Baret F, de Solan B, Thomas S, Dutartre D, Jezequel S, Hemmerlé M, Colombeau G, Comar A (2017) High-Throughput Phenotyping of Plant Height: Comparing Unmanned Aerial Vehicles and Ground LiDAR Estimates. Frontiers in Plant Science **8:** 2002

Madec S, Jin X, Lu H, De Solan B, Liu S, Duyme F, Heritier E, Baret F (2019) Ear density estimation from high resolution RGB imagery using deep learning technique. Agricultural and Forest Meteorology **264:** 225-234

Marquardt DWJJotsfI, Mathematics A (1963) An algorithm for least-squares estimation of nonlinear parameters. Journal of the society for Industrial and Applied Mathematics **11:** 431-441

Martre P, Dambreville A (2018) A Model of Leaf Coordination to Scale-Up Leaf Expansion from the Organ to the Canopy. Plant Physiology **176:** 704-716

Masle J (1985) Competition Among Tillers in Winter Wheat: Consequences for Growth and Development of the Crop. *In* W Day, RK Atkin, eds, Wheat Growth and Modelling. Springer US, Boston, MA, pp 33-54

Masle J, Doussinault G, Farquhar GD, Sun B (1989) Foliar stage in wheat correlates better to photothermal time than to thermal time. Plant, Cell and Environment **12:** 235-247

Masters T (1993) Practical neural network recipes in C++. Morgan Kaufmann

Miralles DJ, Richards RA (2000) Responses of leaf and tiller emergence and primordium initiation in wheat and barley to interchanged photoperiod. Annals of Botany **85:** 655-663

Monneveux P, Jing R, Misra SC (2012) Phenotyping for drought adaptation in wheat using physiological traits. Frontiers in Physiology **3:** 429

Moulin S, Bondeau A, Delecolle R (1998) Combining agricultural crop models and satellite observations: from field to regional scales. International Journal of Remote Sensing **19:** 1021-1036

Nerson H (1980) Effects of population density and number of ears on wheat yield and its components. Field Crops Research **3:** 225-234

Paproki A, Sirault X, Berry S, Furbank R, Fripp J (2012) A novel mesh processing based technique for 3D plant analysis. BMC Plant Biology **12:** 63

Pradal C, Boudon F, Nouguier C, Chopard J, Godin C (2009) PlantGL: A Python-based geometric library for 3D plant modelling at different scales. Graphical Models **71:** 1-21

Pradal C, Dufour-Kowalski S, Boudon F, Fournier C, Godin C (2008) OpenAlea: a visual programming and component-based software platform for plant modelling. Functional Plant Biology **35:** 751-760

Prado SA, Cabrera-Bosquet L, Grau A, Coupel-Ledru A, Millet EJ, Welcker C, Tardieu F (2018) Phenomics allows identification of genomic regions affecting maize stomatal conductance with conditional effects of water deficit and evaporative demand. Plant, Cell & Environment **41:** 314-326

Rutkoski J, Poland J, Mondal S, Autrique E, Perez LG, Crossa J, Reynolds M, Singh R (2016) Canopy Temperature and Vegetation Indices from High-Throughput Phenotyping Improve Accuracy of Pedigree and Genomic Selection for Grain Yield in Wheat. G3 (Bethesda) **6:** 2799-2808

Schirrmann M, Giebel A, Gleiniger F, Pflanz M, Lentschke J, Dammer K-H (2016) Monitoring Agronomic Parameters of Winter Wheat Crops with Low-Cost UAV Imagery. Remote Sensing **8:** 706

Tardieu F, Tuberosa R (2010) Dissection and modelling of abiotic stress tolerance in plants. Current Opinion in Plant Biology **13:** 206-212

Vos J, Evers JB, Buck-Sorlin GH, Andrieu B, Chelle M, Visser PHBd (2010) Functional–structural plant modelling: a new versatile tool in crop science. Journal of Experimental Botany **61:** 2101-2115

Weiss M, Troufleau D, Baret F, Chauki H, Prévot L, Olioso A, Bruguier N, Brisson N (2001) Coupling canopy functioning and canopy radiative transfer models for remote sensing data assimilation. Agricultural and Forest Meteorology **108:** 113-128

Whaley J, Sparkes D, Foulkes M, Spink J, Semere T, Scott R (2000) The physiological response of winter wheat to reductions in plant density. Annals of Applied Biology **137:** 165-177

White JW, Conley MM (2013) A Flexible, Low-Cost Cart for Proximal Sensing. Crop science. **53:** 1646-1649

Widlowski JL, Robustelli M, Disney M, Gastellu-Etchegorry JP, Lavergne T, Lewis P, North PRJ, Pinty B, Thompson R, Verstraete MM (2008) The RAMI On-line Model Checker (ROMC): A web-based benchmarking facility for canopy reflectance models. Remote Sensing of Environment **112:** 1144-1150

Zhang L, Guo CL, Zhao LY, Zhu Y, Cao WX, Tian YC, Cheng T, Wang X (2016) Estimating wheat yield by integrating the WheatGrow and PROSAIL models. Field Crops Research **192:** 55-66

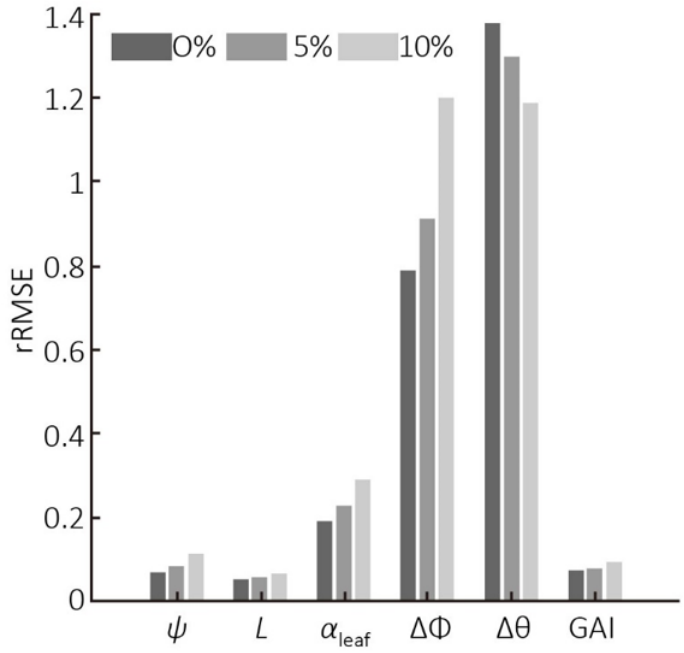

Fig. 1 Relative root mean squared error (rRMSE) for five parameters of ADEL-Wheat and green area index (GAI) estimated with the Digital Plant Phenotyping Platform using the green fraction observations under five view directions for five dates before tillering. Three levels of noise were considered (0%, 5% and 10%) for the evaluation dataset. The five parameters are: ψ, phyllochron; L, laminae length of leaf 1, rank from the bottom; α_{leaf}, increase rate of lamina length; $\Delta\varphi$, standard deviation of the leaf azimuth compared to the previous one with mean 180°; $\Delta\theta$, shift of leaf basal inclination.

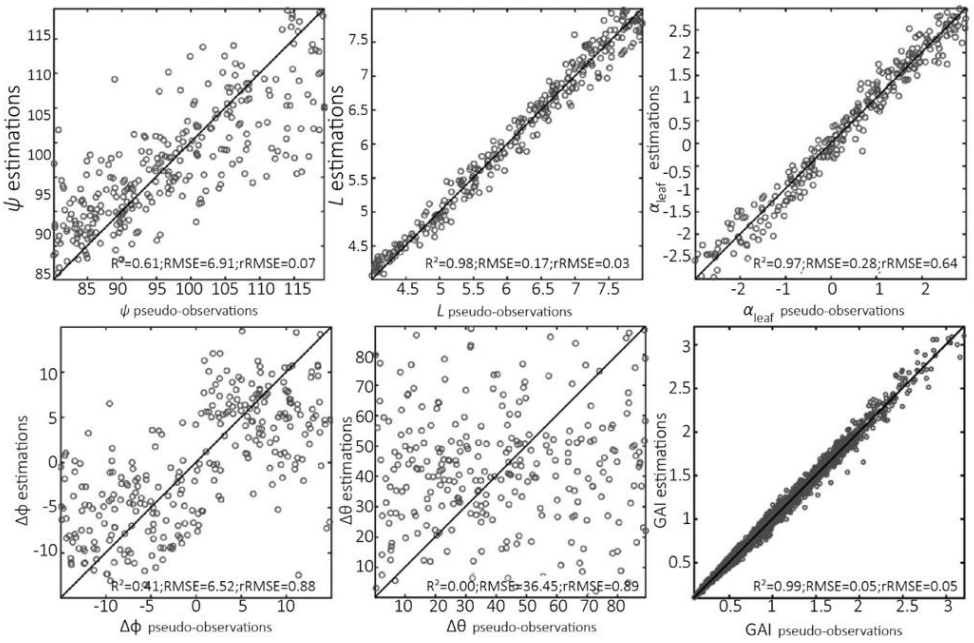

Fig. 2 Comparison of the estimated and pseudo-observation values of the five parameters of ADEL-Wheat and the green area index (GAI) computed for the five dates of green fraction (GF) measurements with the reference values for the first growth period (between crop emergence and ligulation of leaf 3). Synthetic GF data were obtained from five view directions with 5% noise. The five parameters are: N_{sen}, number of green leaves at the start of leaf senescence on the mainstem; N_{min}, minimum number of green leaves on the mainstem; N_{til}, final number of tillers per plant; θ_{til}, inclination of the base of tillers relative to mainstem inclination; α_{til}, change of tiller inclination angle with the number of emerged leaves.

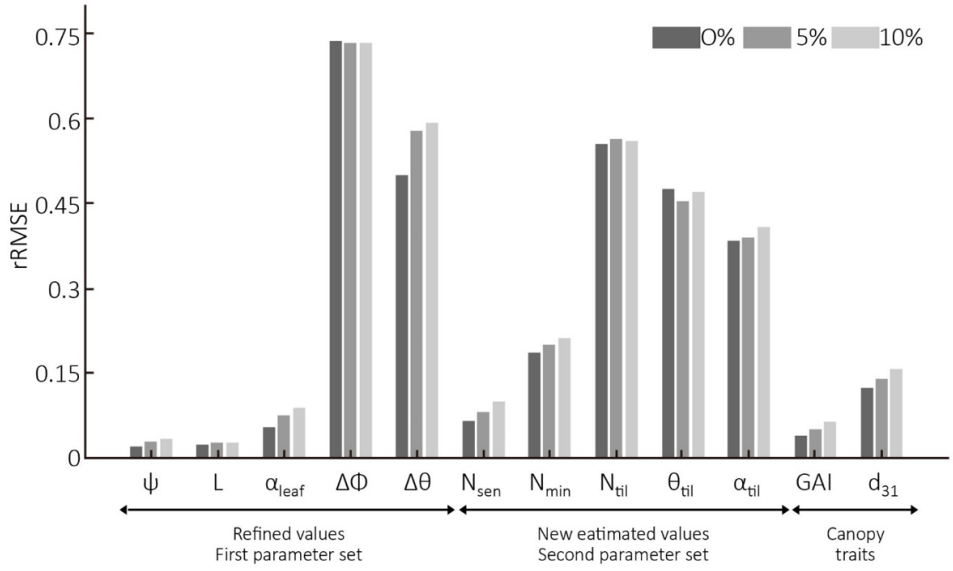

Fig. 3 Relative root mean squared error (rRMSE) for ten parameters of ADEL-Wheat, green area index (GAI), and the number of tillers with at least three leaves at the beginning of stem elongation (d_{3l}) estimated with the Digital Plant Phenotyping Platform using the green fraction observations under five view directions for 10 dates between crop emergence and the beginning of stem elongation. Three levels of noise were considered (0%, 5% and 10%) for the evaluation dataset. The ten parameters include: ψ, phyllochron; L, laminae length of leaf 1, rank from the bottom; α_{leaf}, increase rate of lamina length; $\Delta\varphi$, standard deviation of the leaf azimuth compared to the previous one with mean 180°; $\Delta\theta$, shift of leaf basal inclination N_{sen}, number of green leaves at the start of leaf senescence on the mainstem; N_{min}, minimum number of green leaves on the mainstem; N_{til}, final number of tillers per plant; θ_{til}, inclination of the base of tillers relative to mainstem inclination; α_{til}, change of tiller inclination angle with the number of emerged leaves.

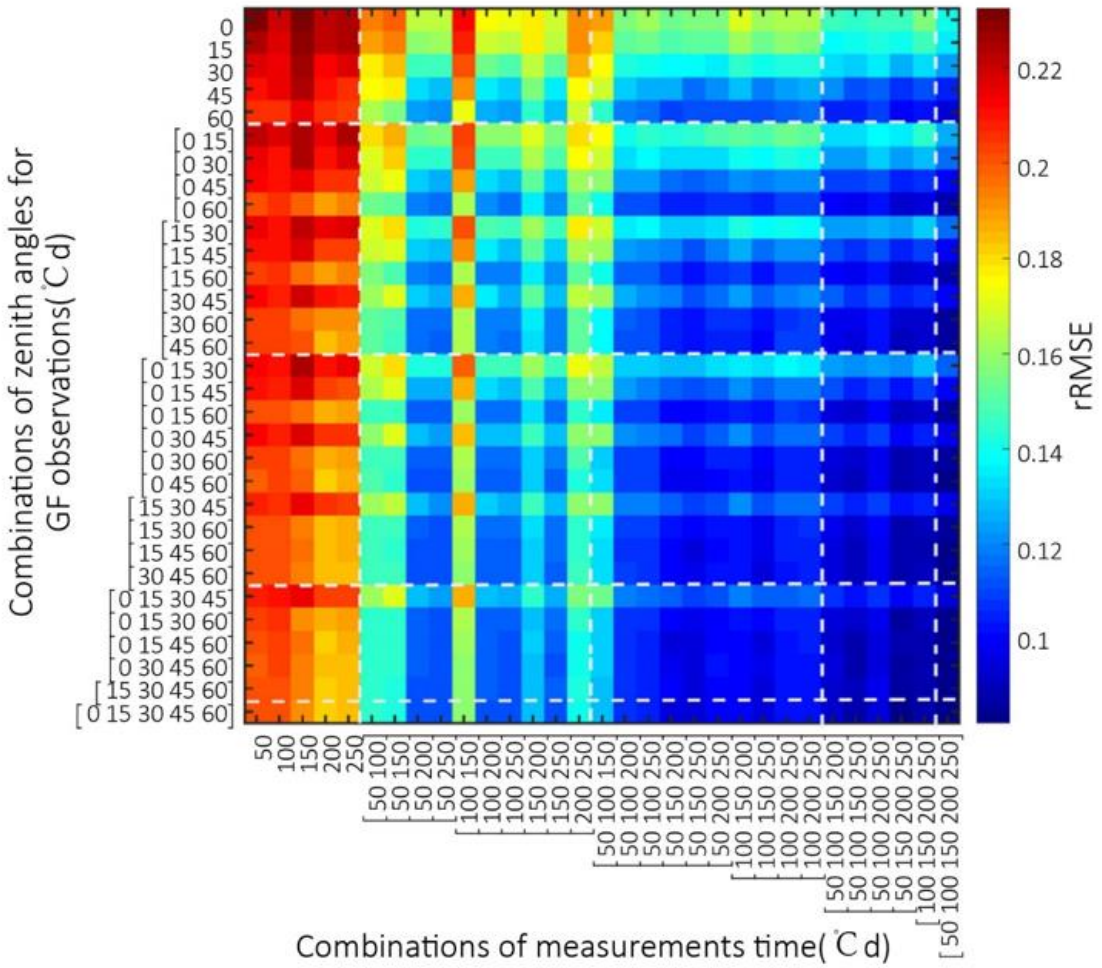

Fig. 4 Average relative root mean squared error (rRMSE) for the three estimated ADEL-Wheat parameters ($\psi, L,$ and α_{leaf}) and GAI obtained from the 961 combinations of one to five directions and one to five dates before tillering.

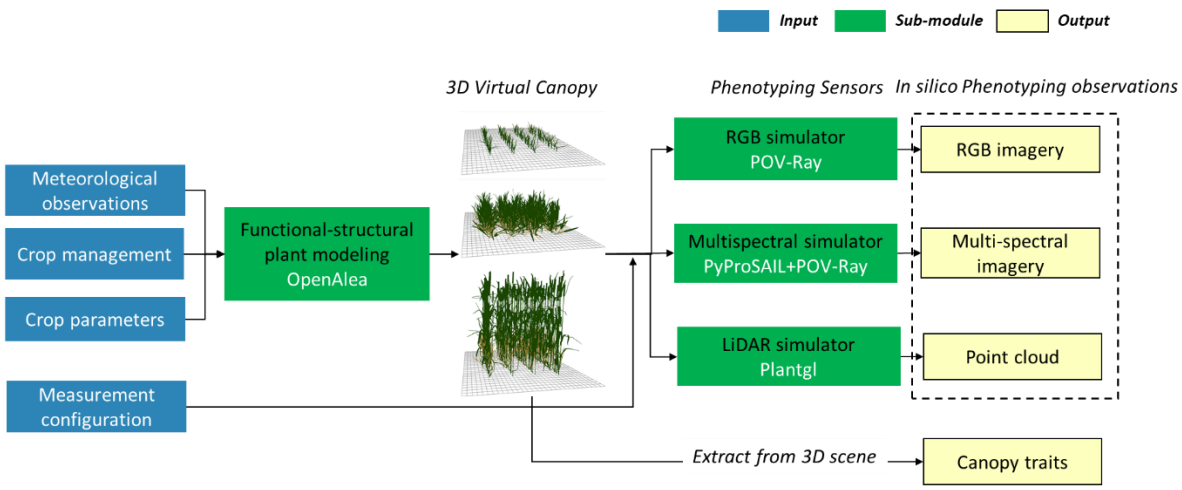

Fig. 5 Schema of the Digital Plant Phenotyping Platform (D3P) that simulates phenotyping observations from environmental variables, crop management and meteorological information

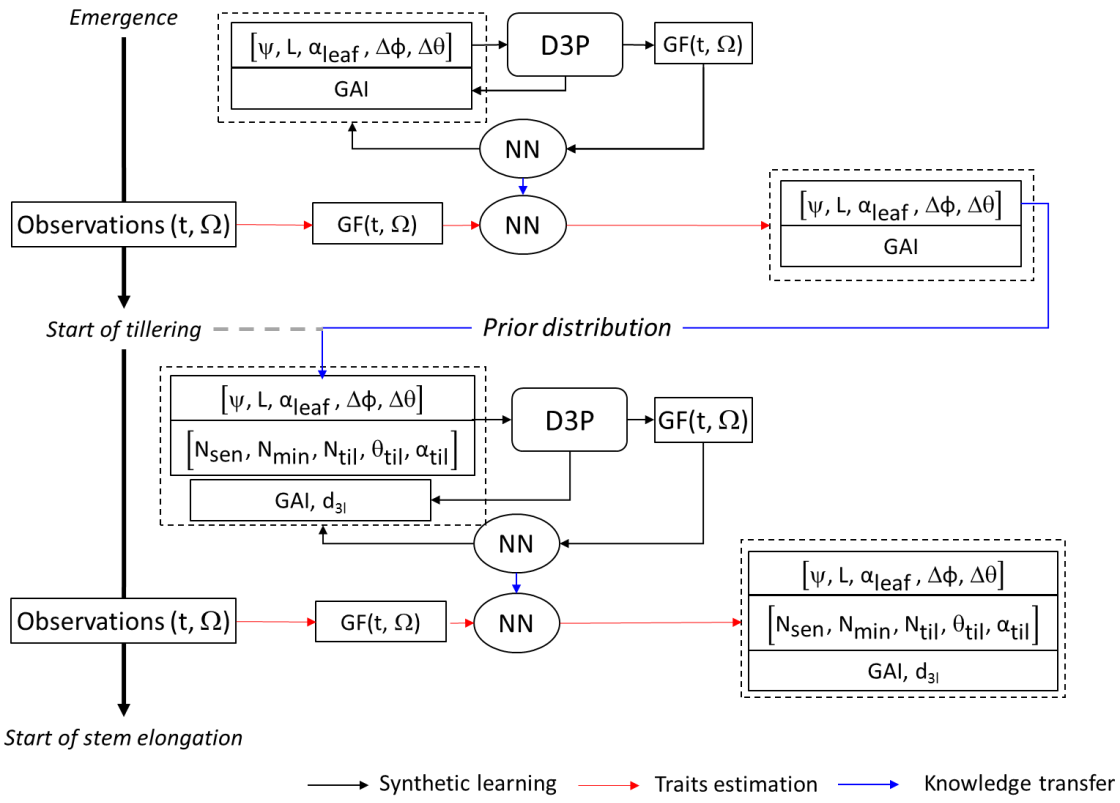

Fig. 6 Diagram showing the sequential scheme of green fraction assimilation. The assimilation was done in two consecutive steps: between crop emergence and the start of tillering (before tillering), and between crop emergence and the beginning of stem elongation (before stem elongation). In each step, a neural network (NN) was first trained using the training green fraction (GF(t,Ω)) dataset. The trained NN was then used to estimate ADEL-Wheat parameters and GAI using the green fraction (GF(t,Ω)) validation dataset. The distribution of ADEL-Wheat parameters estimated in the first step (before tillering) were used as prior information when training the NN in the second step (before stem elongation). Finally, the tiller number with more than three leaves at the beginning of stem elongation (d_{3l}) was computed from the estimated set of parameters.

Parsed Citations

Abichou M (2016) Modélisation de l'architecture 4D du blé : identification des patterns dans la morphologie, la sénescence et le positionnement spatial des organes dans une large gamme de situations de croissance. AgroParisTech, Université Paris-Saclay, Paris
Pubmed: Author and Title
Google Scholar: Author Only Title Only Author and Title

Abichou M, Fournier C, Dornbusch T, Chambon C, Baccar R, Bertheloot J, Vidal T, Robert C, David G, Andrieu B (2013) Re-parametrisation of Adel-wheat allows reducing the experimental effort to simulate the 3D development of winter wheat. In Proceedings of the 7th International Conference on Functional-Structural Plant Models, pp 304–306
Pubmed: Author and Title
Google Scholar: Author Only Title Only Author and Title

Abichou M, Fournier C, Dornbusch T, Chambon C, de Solan B, Gouache D, Andrieu B (2018) Parameterising wheat leaf and tiller dynamics for faithful reconstruction of wheat plants by structural plant models. Field Crops Research 218: 213-230
Pubmed: Author and Title
Google Scholar: Author Only Title Only Author and Title

Araus J, Amaro T, Zuhair Y, Nachit M (1997) Effect of leaf structure and water status on carbon isotope discrimination in field grown durum wheat. Plant, Cell & Environment 20: 1484-1494
Pubmed: Author and Title
Google Scholar: Author Only Title Only Author and Title

Bacour C, Peylin P, MacBean N, Rayner PJ, Delage F, Chevallier F, Weiss M, Demarty J, Santaren D, Baret F, Berveiller D, Dufrene E, Prunet P (2015) Joint assimilation of eddy covariance flux measurements and FAPAR products over temperate forests within a process-oriented biosphere model. Journal of Geophysical Research-Biogeosciences 120: 1839-1857
Pubmed: Author and Title
Google Scholar: Author Only Title Only Author and Title

Baret F, Buis S (2008) Estimating canopy characteristics from remote sensing observations: Review of methods and associated problems. In Advances in land remote Sensing. Springer, pp 173–201
Pubmed: Author and Title
Google Scholar: Author Only Title Only Author and Title

Baret F, de Solan B, Lopez-Lozano R, Ma K, Weiss M (2010) GAI estimates of row crops from downward looking digital photos taken perpendicular to rows at 57.5{degree sign} zenith angle: Theoretical considerations based on 3D architecture models and application to wheat crops. Agricultural and Forest Meteorology 150: 1393-1401
Pubmed: Author and Title
Google Scholar: Author Only Title Only Author and Title

Baumont M, Parent B, Manceau L, Brown H, Driever SM, Muller B, Martre P (2019) Experimental and modeling evidence of carbon limitation of leaf appearance rate for spring and winter wheat. Journal of Experimental Botany 70: 2449-2462
Pubmed: Author and Title
Google Scholar: Author Only Title Only Author and Title

Bustos-Korts D (2017) Modelling of genotype by environment interaction and prediction of complex traits across multiple environments as a synthesis of crop growth modelling, genetics and statistics. Wageningen University, Wageningen
Pubmed: Author and Title
Google Scholar: Author Only Title Only Author and Title

Cabrera Bosquet L, Fournier C, Brichet N, Welcker C, Suard B, Tardieu F (2016) High throughput estimation of incident light, light interception and radiation use efficiency of thousands of plants in a phenotyping platform. New Phytologist 212: 269-281
Pubmed: Author and Title
Google Scholar: Author Only Title Only Author and Title

Cao W, Moss DN (1989) Temperature and daylength interaction on phyllochron in wheat and barley. Crop Science 29: 1046–1048
Pubmed: Author and Title
Google Scholar: Author Only Title Only Author and Title

Comar A, Burger P, de Solan B, Baret F, Daumard F, Hanocq JF (2012) A semi-automatic system for high throughput phenotyping wheat cultivars in-field conditions: description and first results. Journal of Functional Biology 39: 914-924
Pubmed: Author and Title
Google Scholar: Author Only Title Only Author and Title

Combal B, Baret F, Weiss M, Trubuil A, Macé D, Pragnère A, Myneni R, Knyazikhin Y, Wang L (2003) Retrieval of canopy biophysical variables from bidirectional reflectance. Remote Sensing of Environment 84: 1-15
Pubmed: Author and Title
Google Scholar: Author Only Title Only Author and Title

Dornbusch T, Andrieu B (2010) Lamina2Shape-An image processing tool for an explicit description of lamina shape tested on winter wheat (Triticum aestivum L.). Computers and Electronics in Agriculture 70: 217-224
Pubmed: Author and Title
Google Scholar: Author Only Title Only Author and Title

Duan T, Chapman S, Holland E, Rebetzke G, Guo Y, Zheng B (2016) Dynamic quantification of canopy structure to characterize early plant vigour in wheat genotypes. Journal of Experimental Botany 67: 4523-4534
Pubmed: Author and Title
Google Scholar: Author Only Title Only Author and Title

Edmeades GO (1996) Developing Drought and Low N-tolerant Maize: Proceedings of a Symposium, March 25-29, 1996, CIMMYT, El Batán, Mexico. CIMMYT
Pubmed: Author and Title
Google Scholar: Author Only Title Only Author and Title

Evers JB, Vos J, Andrieu B, Struik PC (2006) Cessation of tillering in spring wheat in relation to light interception and red : far-red ratio. Annals of Botany 97: 649-658
Pubmed: Author and Title
Google Scholar: Author Only Title Only Author and Title

Evers JB, Vos J, Fournier C, Andrieu B, Chelle M, Struik PC (2005) Towards a generic architectural model of tillering in Gramineae, as exemplified by spring wheat (Triticum aestivum). New Phytologist 166: 801-812
Pubmed: Author and Title
Google Scholar: Author Only Title Only Author and Title

Fournier C, Andrieu B (1999) ADEL-maize: an L-system based model for the integration of growth processes from the organ to the canopy. Application to regulation of morphogenesis by light availability. Agronomie 19: 313–327
Pubmed: Author and Title
Google Scholar: Author Only Title Only Author and Title

Fournier C, Andrieu B, Ljutovac S, Saint-Jean S (2003) ADEL-wheat: a 3D architectural model of wheat development. Proceedings of the 2003 Plant Growth Modeling, Simulation, Visualization, and Applications: 54–63
Pubmed: Author and Title
Google Scholar: Author Only Title Only Author and Title

Gibbs JA, Pound M, French AP, Wells DM, Murchie E, Pridmore T (2017) Approaches to three-dimensional reconstruction of plant shoot topology and geometry. Functional Plant Biology 44: 62-75
Pubmed: Author and Title
Google Scholar: Author Only Title Only Author and Title

Govaerts YM, Verstraete MM (1998) Raytran: A Monte Carlo ray-tracing model to compute light scattering in three-dimensional heterogeneous media. Ieee Transactions on Geoscience and Remote Sensing 36: 493-505
Pubmed: Author and Title
Google Scholar: Author Only Title Only Author and Title

Guo W, Rage UK, Ninomiya S (2013) Illumination invariant segmentation of vegetation for time series wheat images based on decision tree model. Computers and Electronics in Agriculture 96: 58-66
Pubmed: Author and Title
Google Scholar: Author Only Title Only Author and Title

Hafsi M, Akhter J, Monneveux P (2007) Leaf senescence and carbon isotope discrimination in durum wheat (Triticum durum Desf.) under severe drought conditions. Cereal Research Communications 35: 71-80
Pubmed: Author and Title
Google Scholar: Author Only Title Only Author and Title

Hammer G, Cooper M, Tardieu F, Welch S, Walsh B, van Eeuwijk F, Chapman S, Podlich D (2006) Models for navigating biological complexity in breeding improved crop plants. Trends in Plant Science 11: 587-593
Pubmed: Author and Title
Google Scholar: Author Only Title Only Author and Title

Hartmann A, Czauderna T, Hoffmann R, Stein N, Schreiber F (2011) HTPheno: an image analysis pipeline for high-throughput plant phenotyping. BMC bioinformatics 12: 148
Pubmed: Author and Title
Google Scholar: Author Only Title Only Author and Title

Hay R, Kirby E (1991) Convergence and synchrony-a review of the coordination of development in wheat. Crop and Pasture Science 42: 661-700
Pubmed: Author and Title
Google Scholar: Author Only Title Only Author and Title

He J, Le Gouis J, Stratonovitch P, Allard V, Gaju O, Heumez E, Orford S, Griffiths S, Snape JW, Foulkes MJ, Semenov MA, Martre P (2012) Simulation of environmental and genotypic variations of final leaf number and anthesis date for wheat. European Journal of Agronomy 42: 22-33
Pubmed: Author and Title
Google Scholar: Author Only Title Only Author and Title

Hokmalipour S (2011) The Study of Phyllochron and Leaf Appearance Rate in Three Cultivar of Maize (Zea mays L.) At Nitrogen Fertilizer Levels. World Applied Sciences Journal 12: 850–856
Pubmed: Author and Title
Google Scholar: Author Only Title Only Author and Title

Jacquemoud S, Baret F (1990) PROSPECT: A model of leaf optical properties spectra. Remote sensing of environment 34: 75-91
Pubmed: Author and Title
Google Scholar: Author Only Title Only Author and Title

Jin X, Liu S, Baret F, Hemerlé M, Comar A (2017) Estimates of plant density of wheat crops at emergence from very low altitude UAV imagery. Remote Sensing of Environment 198: 105-114
Pubmed: Author and Title
Google Scholar: Author Only Title Only Author and Title

Kimes DS, Knyazikhin Y, Privette JL, Abuelgasim AA, Gao F (2000) Inversion methods for physically-based models. Remote Sensing Reviews 18: 381-439
Pubmed: Author and Title
Google Scholar: Author Only Title Only Author and Title

Kirby EJM, Appleyard M, Fellowes G (1985) Leaf emergence and tillering in barley and wheat. Agronomie 5: 193–200
Pubmed: Author and Title
Google Scholar: Author Only Title Only Author and Title

Ledent JF, Moss DN (1977) Spatial orientation of wheat leaves. Crop Science 17: 873–879
Pubmed: Author and Title
Google Scholar: Author Only Title Only Author and Title

Li W, Weiss M, Waldner F, Defourny P, Demarez V, Morin D, Hagolle O, Baret F (2015) A Generic Algorithm to Estimate LAI, FAPAR and FCOVER Variables from SPOT4_HRVIR and Landsat Sensors: Evaluation of the Consistency and Comparison with Ground Measurements. Remote Sensing 7: 15494-15516
Pubmed: Author and Title
Google Scholar: Author Only Title Only Author and Title

Liu S, Baret F, Abichou M, Boudon F, Thomas S, Zhao K, Fournier C, Andrieu B, Irfan K, Hemmerlé M, de Solan B (2017) Estimating wheat green area index from ground-based LiDAR measurement using a 3D canopy structure model. Agricultural and Forest Meteorology 247: 12-20
Pubmed: Author and Title
Google Scholar: Author Only Title Only Author and Title

Liu S, Baret F, Andrieu B, Abichou M, Allard D, de Solan B, Burger P (2017) Modeling the spatial distribution of plants on the row for wheat crops: Consequences on the green fraction at the canopy level. Computers and Electronics in Agriculture 136: 147-156
Pubmed: Author and Title
Google Scholar: Author Only Title Only Author and Title

Liu S, Baret F, Andrieu B, Burger P, Hemmerle M (2017) Estimation of Wheat Plant Density at Early Stages Using High Resolution Imagery. Frontiers in Plant Science 8: 739
Pubmed: Author and Title
Google Scholar: Author Only Title Only Author and Title

López-Lozano R, Baret F, Chelle M, Rochdi N, España M (2007) Sensitivity of gap fraction to maize architectural characteristics based on 4D model simulations. Agricultural and Forest Meteorology 143: 217-229
Pubmed: Author and Title
Google Scholar: Author Only Title Only Author and Title

Lopez-Lozano R, Baret F, García de Cortázar-Atauri I, Bruguier N, Casterad MA (2009) Optimal geometric configuration and algorithms for LAI indirect estimates under row canopies. The case of vineyards. Agricultural and Forest Meteorology 149: 1309-1316
Pubmed: Author and Title
Google Scholar: Author Only Title Only Author and Title

Maddonni GA, Chelle M, Drouet JL, Andrieu B (2001) Light interception of contrasting azimuth canopies under square and rectangular plant spatial distributions: simulations and crop measurements. Field Crops Research 70: 1-13
Pubmed: Author and Title
Google Scholar: Author Only Title Only Author and Title

Madec S, Baret F, de Solan B, Thomas S, Dutartre D, Jezequel S, Hemmerlé M, Colombeau G, Comar A (2017) High-Throughput Phenotyping of Plant Height: Comparing Unmanned Aerial Vehicles and Ground LiDAR Estimates. Frontiers in Plant Science 8: 2002
Pubmed: Author and Title
Google Scholar: Author Only Title Only Author and Title

Madec S, Jin X, Lu H, De Solan B, Liu S, Duyme F, Heritier E, Baret F (2019) Ear density estimation from high resolution RGB imagery using deep learning technique. Agricultural and Forest Meteorology 264: 225-234
Pubmed: Author and Title
Google Scholar: Author Only Title Only Author and Title

Marquardt DWJJotsfI, Mathematics A (1963) An algorithm for least-squares estimation of nonlinear parameters. Journal of the society for Industrial and Applied Mathematics 11: 431-441
Pubmed: Author and Title
Google Scholar: Author Only Title Only Author and Title

Martre P, Dambreville A (2018) A Model of Leaf Coordination to Scale-Up Leaf Expansion from the Organ to the Canopy. Plant Physiology 176: 704-716
Pubmed: Author and Title
Google Scholar: Author Only Title Only Author and Title

Masle J (1985) Competition Among Tillers in Winter Wheat: Consequences for Growth and Development of the Crop. In W Day, RK Atkin, eds, Wheat Growth and Modelling. Springer US, Boston, MA, pp 33-54
Pubmed: Author and Title
Google Scholar: Author Only Title Only Author and Title

Masle J, Doussinault G, Farquhar GD, Sun B (1989) Foliar stage in wheat correlates better to photothermal time than to thermal time. Plant, Cell and Environment 12: 235-247
Pubmed: Author and Title
Google Scholar: Author Only Title Only Author and Title

Masters T (1993) Practical neural network recipes in C++. Morgan Kaufmann
Pubmed: Author and Title
Google Scholar: Author Only Title Only Author and Title

Miralles DJ, Richards RA (2000) Responses of leaf and tiller emergence and primordium initiation in wheat and barley to interchanged photoperiod. Annals of Botany 85: 655-663
Pubmed: Author and Title
Google Scholar: Author Only Title Only Author and Title

Monneveux P, Jing R, Misra SC (2012) Phenotyping for drought adaptation in wheat using physiological traits. Frontiers in Physiology 3: 429
Pubmed: Author and Title
Google Scholar: Author Only Title Only Author and Title

Moulin S, Bondeau A, Delecolle R (1998) Combining agricultural crop models and satellite observations: from field to regional scales. International Journal of Remote Sensing 19: 1021-1036
Pubmed: Author and Title
Google Scholar: Author Only Title Only Author and Title

Nerson H (1980) Effects of population density and number of ears on wheat yield and its components. Field Crops Research 3: 225-234
Pubmed: Author and Title
Google Scholar: Author Only Title Only Author and Title

Paproki A, Sirault X, Berry S, Furbank R, Fripp J (2012) A novel mesh processing based technique for 3D plant analysis. BMC Plant Biology 12: 63
Pubmed: Author and Title
Google Scholar: Author Only Title Only Author and Title

Pradal C, Boudon F, Nouguier C, Chopard J, Godin C (2009) PlantGL: A Python-based geometric library for 3D plant modelling at different scales. Graphical Models 71: 1-21
Pubmed: Author and Title
Google Scholar: Author Only Title Only Author and Title

Pradal C, Dufour-Kowalski S, Boudon F, Fournier C, Godin C (2008) OpenAlea: a visual programming and component-based software platform for plant modelling. Functional Plant Biology 35: 751-760
Pubmed: Author and Title
Google Scholar: Author Only Title Only Author and Title

Prado SA, Cabrera-Bosquet L, Grau A, Coupel-Ledru A, Millet EJ, Welcker C, Tardieu F (2018) Phenomics allows identification of genomic regions affecting maize stomatal conductance with conditional effects of water deficit and evaporative demand. Plant, Cell & Environment 41: 314-326
Pubmed: Author and Title
Google Scholar: Author Only Title Only Author and Title

Rutkoski J, Poland J, Mondal S, Autrique E, Perez LG, Crossa J, Reynolds M, Singh R (2016) Canopy Temperature and Vegetation Indices from High-Throughput Phenotyping Improve Accuracy of Pedigree and Genomic Selection for Grain Yield in Wheat. G3 (Bethesda) 6: 2799-2808
Pubmed: Author and Title
Google Scholar: Author Only Title Only Author and Title

Schirrmann M, Giebel A, Gleiniger F, Pflanz M, Lentschke J, Dammer K-H (2016) Monitoring Agronomic Parameters of Winter Wheat Crops with Low-Cost UAV Imagery. Remote Sensing 8: 706
Pubmed: Author and Title
Google Scholar: Author Only Title Only Author and Title

Tardieu F, Tuberosa R (2010) Dissection and modelling of abiotic stress tolerance in plants. Current Opinion in Plant Biology 13: 206-212
Pubmed: Author and Title
Google Scholar: Author Only Title Only Author and Title

Vos J, Evers JB, Buck-Sorlin GH, Andrieu B, Chelle M, Visser PHBd (2010) Functional–structural plant modelling: a new versatile tool in crop science. Journal of Experimental Botany 61: 2101-2115
Pubmed: Author and Title
Google Scholar: Author Only Title Only Author and Title

Weiss M, Troufleau D, Baret F, Chauki H, Prévot L, Olioso A, Bruguier N, Brisson N (2001) Coupling canopy functioning and canopy radiative transfer models for remote sensing data assimilation. Agricultural and Forest Meteorology 108: 113-128
Pubmed: Author and Title
Google Scholar: Author Only Title Only Author and Title

Whaley J, Sparkes D, Foulkes M, Spink J, Semere T, Scott R (2000) The physiological response of winter wheat to reductions in plant density. Annals of Applied Biology 137: 165-177
Pubmed: Author and Title
Google Scholar: Author Only Title Only Author and Title

White JW, Conley MM (2013) A Flexible, Low-Cost Cart for Proximal Sensing. Crop science. 53: 1646-1649
Pubmed: Author and Title
Google Scholar: Author Only Title Only Author and Title

Widlowski JL, Robustelli M, Disney M, Gastellu-Etchegorry JP, Lavergne T, Lewis P, North PRJ, Pinty B, Thompson R, Verstraete MM (2008) The RAMI On-line Model Checker (ROMC): A web-based benchmarking facility for canopy reflectance models. Remote Sensing of Environment 112: 1144-1150
Pubmed: Author and Title
Google Scholar: Author Only Title Only Author and Title

Zhang L, Guo CL, Zhao LY, Zhu Y, Cao WX, Tian YC, Cheng T, Wang X (2016) Estimating wheat yield by integrating the WheatGrow and PROSAIL models. Field Crops Research 192: 55-66
Pubmed: Author and Title
Google Scholar: Author Only Title Only Author and Title